7 YEARS OF AVALANCHE MEASUREMENTS WITH THE GEODAR RADAR SYSTEM

Anselm Köhler[1,2,*], Betty Sovilla[1], Jim McElwaine[2]

[1] WSL Institute for Snow and Avalanche Research SLF, Davos, Switzerland
[2] University of Durham, Durham, United Kingdom

ABSTRACT: Observations of snow avalanches using radar are becoming more and more common in the daily work of practitioners and their scientific uses are also increasing. Radar systems have two great strengths: They can operate in any weather conditions and they can penetrate the powder cloud and measure the underlying dense flow (if the wavelength is larger than a few mm.) This underlying dense flow is nearly always the most destructive part of an avalanche except for the very largest.

The GEODAR radar system was first installed for the winter season 2010–2011 at the avalanche test site Vallée de la Sionne in Canton Valais, Switzerland. Since then more than 200 avalanches of all sizes and flow types have been captured. The data show many different types of flow characteristics and have been used to develop a comprehensive classification of avalanche flow regimes. For the first time, the evolution of flow regimes and the transitions between them can be recorded along the full avalanche path with a spatial resolution of 0.75 m at around 100 Hz. This new information points out again the huge complexity of snow avalanches and the data will prove invaluable in validating and developing avalanche models.

Keywords: Avalanche dynamics, Radar measurements, Flow regime, GEODAR data repository

1. INTRODUCTION

The GEODAR (GEOphysical flow dynamics using pulsed Doppler radAR) radar system was purpose-built for imaging geophysical flows such as snow avalanches. The hardware was developed by Matthew Ash under the supervision of Paul Brennan (Ash, 2013) and has developed through five versions. GEODAR is designed for scientific data gathering and the data is processed off-line, but as technology improves and costs fall it could be used for real-time monitoring at reasonable cost.

The first data processing and interpretation were published by Vriend et al. (2013), and immediately gave an unprecedented look into the heart of a flowing avalanche. Since then the processing has steadily advanced (Köhler, 2018), and a comprehensive interpretation of the data has been achieved and published in a series of papers: Köhler et al. (2018b) identified seven distinct flowing regimes which can occur, sometimes all within a single avalanche; Köhler et al. (2016) showed that internal surges and flow features can move at twice the speed of the front; Köhler et al. (2018a) gave a detailed description of the cold-to-warm flow regime transition that frequently occurs as an avalanche moves down a mountain. Recently, Faug et al.

(2018) commented on these findings and pointed out the future usefulness of the GEODAR data for the development of the next generation of avalanche models.

This extended abstract summarizes the last seven years of GEODAR measurements. This includes an overview of the scientific results, a discussion of future data interpretation for model calibration and ideas for improvements of the radar hardware and software processing.

2. THE RADAR SYSTEM GEODAR

GEODAR is a frequency modulated continuous wave (FMCW) system, which offers fine spatial resolution at a reasonable transmission power (Ash, 2013). Currently, the system operates with a resolution of 0.75 m in range (distance along line of sight) at a frequency of 111 Hz.

The radar system has been in Vallée de la Sionne since the winter season 2010/11. It is mounted close to the valley bottom to ensure measurements with a slope parallel line of sight. The release area is at a range of up to 2800 m, the avalanche track divides into two steep couloirs at a range of 1500 m, the deposit area starts at 1000 m range and the valley ground is reached at 150 m (Vriend et al., 2013).

The radar hardware is modular and built from off-the-shelf microwave components (Ash, 2013). This has two main advantages: failing components can be replaced easily and modules can be individually

*Corresponding author address: WSL Institute for Snow and Avalanche Research SLF, Flüelastrasse 11, CH-7260 Davos, Switzerland, email: anselm.koehler@gmail.com
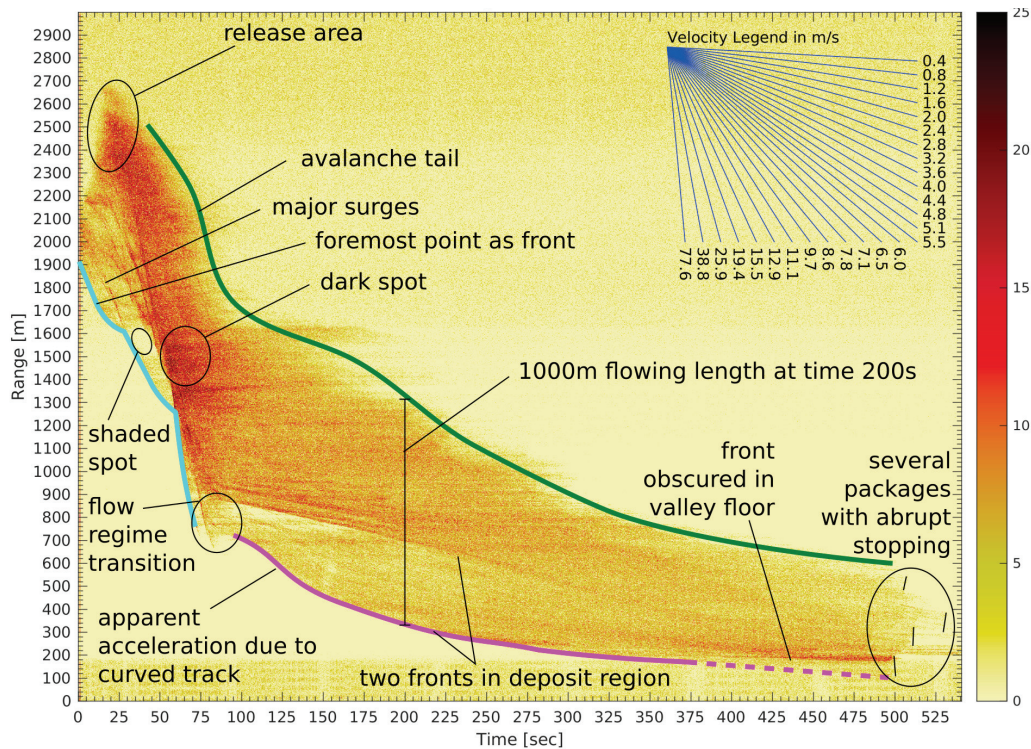
Figure 1: GEODAR data as MTI image of a full scale avalanche (#18-3066). The avalanche front is highlighted in turquoise (cold snow) and pink (warm snow), and the tail is indicated by the green line. Annotations are placed at typical signatures which can be found often in the data (see sec. 3.1).

upgraded. All the modules are protected inside a concrete bunker apart from the antennas, which are outside and exposed to an avalanche impact. They are standard WiFi antennas and can be cheaply replaced, but so far have only been destroyed once.

The range resolution is determined by the bandwidth (200 MHz) and the maximum range and time resolution by the chirp repetition rate. The current system uses a single set of 4 ms up and down chirps. In theory this allows both range and velocity (using the Doppler effect), to be calculated, but this is extremely complicated for a distributed target and so far only range analysis has been done. Therefore, the range estimation suffers a shift of around 5 m for a target moving at $50 \, \mathrm{m \, s^{-1}}$ (Köhler, 2018, sec. 2.2). Note that the shift is reversed between the up and the down chirps so can in theory be removed.

The raw data, consisting of the output of the mixing stage in the receiver unit for each receive antenna sampled at 2 MHz with 16 bits of precision, are streamed to a RAID system. Therefore, different processing algorithms can be developed and tested to extract specific details. This is a distinct advantage to having the processing in the radar system and only storing the results. However, real-time processing is possible and could be used for detection and warning systems. A detailed description of the software data processing can be found in Köhler (2018, sec. 2.4). The algorithms can be grouped

into chirp extraction, spectral ranging and MTI filtering.

A moving target identification (MTI) filter is used to differentiate between the static background clutter and the moving targets, i.e. the avalanche. The simplest MTI filter is the difference between two consecutive returns. If there were no changes, and no noise, the resulting MTI would be zero, however, a 3 dB MTI noise level is usual. To resolve changes on different time scales, more than two chirp pulses need to be taken into account. We found that a visually good result is achieved using a 150 pulses long finite impulse response filter (McElwaine* et al., 2017). Applying different MTI filters , e.g. a filter-bank, would be an interesting area for future research, especially to detect coherently moving targets like plug flow regions.

3. RADAR DATA AND INTERPRETATION

3.1. MTI images

Figure 1 shows an MTI image of a complete recording. The MTI data are usually represented in a range-time plot where the colours are the MTI values on a logarithmic scale relative to the background MTI noise level. The vertical axis is the range or distance along the line of sight, the horizontal axis is time. Each point in the MTI is an averages across the mountain off all points at a certain range

at a certain time. The extend of the lateral average depends on the directionality of the antenna.

The avalanche front is the lowest point of the flow (highlighted in turquoise) and purple in Fig. 1). Similar the tail is defined by the extent of the furthest moving region (green). The distance between the front and the tail, at a moment in time, is the length of the avalanche, that is around 1000 m at 200 s.

The approach velocity is the slope of a line in the MTI which corresponds to a moving feature, as indicated by the velocity legend. Note that curved tracks in relation to the line of sight can cause apparent accelerations and wrong velocity estimates; pure lateral movements can not be detected.

The MTI values cannot be directly interpreted as snow properties, geometric effects, filters, cable attenuation and many other factors change the magnitude if the signal. Nevertheless, trends can be given. Generally speaking, the larger the avalanche in width and height, the larger the MTI signal. For example, the front and major surges until 50 s in Fig. 1 have a weaker signal than the major surge from the large release at high ranges and thus much more mass is expected to be released from there.

The darkest MTI colours are usually observed at ranges around 1500 m where the avalanche enters one of the steep couloirs and increases in flow height and also turbulent intensity. High velocity and turbulences cause a rapidly varying radar cross-section which gives a high signal in the MTI plot.

Completely blank spots occur when the avalanche disappears behind the terrain or old deposits, but can also be caused by the chosen MTI filter which may cancel coherent movement like the sliding of a plug flow. Furthermore, the type of snow in the avalanche changes the amount of reflected signal. Significant reflections come from particles and clusters of particles larger than the wavelength of around 5 cm. Therefore, cold loose snow avalanches of fine grained fresh snow will give a much weaker signal than warm avalanches which consist of larger granules.

The MTI signals inside an avalanche can be very different, and some examples can be seen in Fig. 2. In panel A and C, the signal is rather homogeneously coloured beside some noise and some horizontal bands (normalization artefacts). In contrast, panel B and D show a streak pattern. Those streaks are either surface undulations of a plug flow (E), or minor surges and clusters of denser material in the frontal region of a powder snow avalanche.

3.2. Flow regimes and avalanche type

Köhler et al. (2018b) did an extensive analysis of multiple avalanche recordings and characterized an avalanche into seven flow regimes. A striking finding

is that these flow regimes can even exist simultaneously in one single avalanche along the path.

The colouring of the MTI images are not always enough to uniquely classify each regime, but in conjunction with the form of the avalanche in the range–time image each regime can be identified. A most notable feature is the stopping signature of the avalanche in the MTI image. Köhler et al. (2018b) characterized these into three main stopping signatures: starving, backward propagating shock and abrupt stopping.

Starving is a progressive decrease in avalanche flowing length and is shown in Fig. 2A. Material is deposited at the avalanche tail, while at the same time, the front continues to flow.

Backward propagating shock is a stop of the avalanche front followed by a progressive piling up of the incoming material and is shown in Fig. 2C. There is an upslope thus backward propagating shock clearly visible in the MTI plots. Note that only the shock wave and no material travels upward (Köhler et al., 2016).

Abrupt stopping is an almost instantaneous stop throughout an entire region and is shown in Fig. 2D. This stopping mechanism is characterized by a nearly vertical signature in the MTI plots and occurs in cohesive snow.

Köhler et al. (2018b) found that the snow temperature is a key parameter to describe which stopping mechanism occurs. Starving happens for snow temperatures colder than $-2\,°C$. Backward propagating shocks occurs for snow temperatures around $-1\,°C$. Abrupt stopping is observed only for $0\,°C$ snow with some liquid water content. Both mechanisms for warm snow temperatures may coexist, however, for gentle slope angles abrupt stopping may be favoured compared to shock formation.

The MTI signature of four of the seven flow regimes are shown in the panels of Fig. 2. The two left panels belong to regimes expressed for cold snow temperatures and the right panels correspond to warm snow temperatures. The threshold between warm and cold is around $-1\,°C$ to $-2\,°C$, that is, when snow granulation starts (Steinkogler et al., 2015). Clearly temperature is not the only parameter to differentiate between the regimes, as usually liquid water content is used to separate them in wet and dry, but also size and terrain are factors to be taken into account.

At least the four flow regimes in Fig. 2 appear to be dynamically important: The *Cold dense regime* (CDR) and the *Intermittent regime* (IR) for cold snow, and the *Warm shear regime* (WSR) and the *Warm plug regime* (WPR) for warm snow.

The *cold dense regime* occurs in small to medium sized avalanches — the typical skier triggered avalanche. These avalanches consist of small grains in solid contact behaving like a dry granular
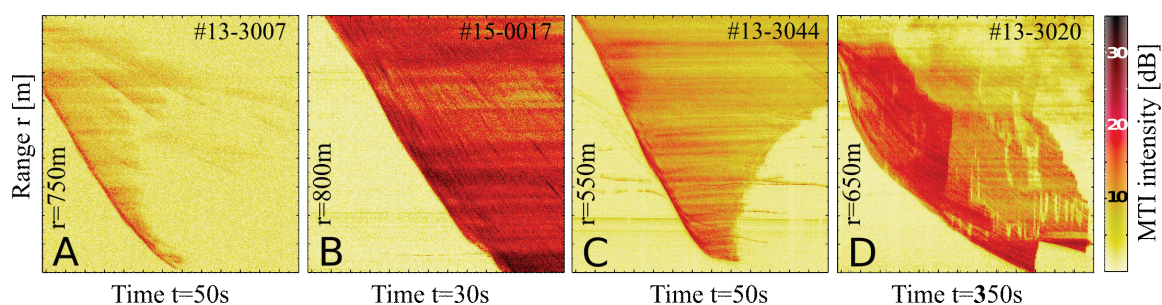
Figure 2: Typical MTI signatures for the avalanche type: A) Cold dense regime, B) Intermittent regime, C) Warm shear regime and D) Warm plug regime. Note: Each panel has a different scale in range and time

flow with negligible influence from the air. The surface of the flow is constantly changing so that the MTI signature is homogeneous. They stop with a starving signature (Fig. 2A).

When such an avalanche grows in size, it develops into a powder snow avalanches with an *intermittent regime*. In this regime particles are not homogeneously distributed but rather aggregated into high density clusters, surrounded by regions of a dilute air-snow mixture (Sovilla et al., 2018). These clusters can be minor surges or mesoscale structures. They show a streak signature in the MTI image and by overtaking the leading edge the clusters give the front a pulsating character (Fig. 2B). The amount of such surging seems to be connected to the avalanche size and its runout (Köhler et al., 2016).

The *warm shear regime* occurs in avalanches where the snow temperature rises above $-1\,°C$ and granules form. The MTI signature is homogeneous, indicating a constantly changing surface of the flow and shearing through the depth (Fig. 2C). The granular nature of this regime is further corroborated by deposition due to piling up of material which requires shearing of the flow (backward propagating shock).

If the temperature of the snow rises even more so that the liquid water content increases, the flow transforms into the *warm plug regime*, i.e. it flows as a series of solid-like pseudo-plugs. The MTI signature reveals parallel streaks (Fig. 2D), probably corresponding to stable surface undulations which travel over large distances, indicating very little mixing during the flow; that is the surface is unchanged. These flows are much slower than the warm shear regime, but can advance far into the valley floor by self-confining the track into very smooth channels (Issler, 2003). We often observe a transition between warm shear and warm plug regime at the beginning of the shallow deposit region, indicating that steeper terrain may prevent the formation of larger flowing units.

3.3. Example avalanche #18-3066

The GEODAR recording of the avalanche in Figure 1 shows all of the previous mentioned flow regimes in one avalanche. This avalanche released in the morning of the 16th of February 2018 as a cold flow but deposited as a warm flow: a so-called transitional avalanche (Köhler et al., 2018a).

When GEODAR starts recording (0 s), a small fraction of the avalanche is already moving between 1900 m to 2200 m range. A larger mass releases in the following 25 s and results in several surges of which the largest comes from a range of 2650 m. This surge flows in the cold dense regime and shows dark MTI intensity with an homogeneous signature. At around 1500 m and 50 s, the surge reaches maximum velocity and below the dark spot converts to the intermittent regime with a few minor surges barely visible.

At 900 m and 75 s, a strong kink indicates the sudden starving of the cold regimes and the rise of two fronts flowing in the warm plug regime, which continue to glide for another 400 s until they stop abruptly. Parts of the MTI signatures below the range of 900 m are homogeneous rather than striped suggesting the existence of a warm shear regime.

The overview of the full scale recording in Figure 1 does not show all the details which have been discussed with the flow regimes, but they can be seen if regions of the plot are enlarged. For example the minor surges of the intermittent regime have a period of only 1 s (Fig. 2B) and cannot be seen in the complete plot.

3.4. Data repository

The MTI from 2009/10 until 2014/15 is available under open access (McElwaine* et al., 2017). The avalanches are identified by the archive number, e.g. #18-3066 means recording 66 in season 2017/18. The archive contains the processed GEODAR data, namely, the MTI plots, plus some derived data such as 1-D thalweg, the projected trajectory, and the downslope velocity. An attached document

serves as metadata and contains details related to GEODAR.

The data is published to improve the interpretation of the MTI data, namely to develop automatic algorithms to extract the front velocity and improve on image processing techniques to identify the MTI signatures and flow regimes. Finally the data is supposed to spur the calibration and development of avalanche models.

3.5. Model calibration

Model calibration can be done in several ways, and traditionally the front velocity and runout is compared between data and simulation results. However, since the GEODAR data give more precisely the avalanche position and any velocity is inferred by geo-referencing the trajectory to a slope parallel quantity (Köhler et al., 2016), additional uncertainties arise.

We suggest therefore a more direct comparison, where the location of the radar is included into the modelling domain. The simulation output is then taken in the same reference frame as the radar data, and a range–time representation of a synthetic MTI plot is compared to the GEODAR data. The front position, respectively the front velocity, the runout and the avalanche tail can be compared. A suitable measure for the goodness of the simulation can be for example the match of the avalanche area in the MTI image of simulation and data.

Furthermore, a suitable parametrisation of colouring the synthetic MTI plot can be used to compare also the MTI signatures. This then can include dark and light spot, or homogeneous and streaks signatures. However, such a procedure needs more research.

Initial work has been done presented by Rauter and Köhler (2017) using an avalanche model based on openFOAM framework developed by Rauter et al. (2018). This open source model enables a simple interface to adjust the computed output as well as testing different physical implementations.

4. OUTLOOK

This paper highlights some of the achievements of the GEODAR project. The data processing has been advanced to generate high resolution MTI images, however, more advanced data processing is still missing. This is namely the range-Doppler differentiation, a two dimensional MTI representation and exploration of more advanced MTI filters to enable automatic feature classification and extraction of the avalanche front. Such recognition algorithms need to function on time-scales of seconds to several minutes and metres to kilometres.

Until now, the MTI data has been interpreted manually. There is definitely more research needed to extract quantitative data from the absolute MTI values. In the future, model development and calibration will become a key use of the data (Faug et al., 2018). Surely, the GEODAR data must be complemented with measurements from other sensors, which therefore should be published open access as well.

The development of a single channel GEODAR which is tailored to low power consumption and transportability will enable the acquisition of data from other avalanche paths, and other geophysical mass flows. For example, we can imagine high-quality data from recordings of rock-ice avalanches, pyroclastic flows and rockfalls.

5. ACKNOWLEDGEMENTS

REFERENCES

Ash, M. (2013). *FMCW Phased Array Radar for Imaging Snow Avalanches*. PhD thesis, University College London.

Faug, T., Turnbull, B., and Gauer, P. (2018). Looking beyond the powder/dense flow avalanche dichotomy. *J. Geophys. Res.*

Issler, D. (2003). Experimental Information on the Dynamics of Dry-Snow Avalanches. In *Dynamic Response of Granular and Porous Materials under Large and Catastrophic Deformations*. Springer, Berlin, Germany.

Köhler, A. (2018). *High resolution radar imaging of snow avalanches*. PhD thesis, Durham University.

Köhler, A., Fischer, J.-T., Scandroglio, R., Bavay, M., McElwaine, J. N., and Sovilla, B. (2018a). Cold-to-warm flow regime transition in snow avalanches. *Cryosphere Discuss.*

Köhler, A., McElwaine, J. N., and Sovilla, B. (2018b). GEODAR Data and the Flow Regimes of Snow Avalanches. *J. Geophys. Res.*

Köhler, A., McElwaine, J. N., Sovilla, B., Ash, M., and Brennan, P. V. (2016). The dynamics of surges in the 3 February 2015 avalanches in Vallée de la Sionne. *J. Geophys. Res.*

McElwaine*, J. N., Köhler*, A., Sovilla, B., Ash, M., and Brennan, P. V. (2017). GEODAR data of snow avalanches at Vallée de la Sionne: Seasons 2010/11, 2011/12, 2012/13 & 2014/15 [Data set]. Zenodo. *equally contributing authors.

Rauter, M., Kofler, A., Huber, A., and Fellin, W. (2018). faSavage-HutterFOAM 1.0: depth-integrated simulation of dense snow avalanches on natural terrain with OpenFOAM. *Geosci. Model Dev.*

Rauter, M. and Köhler, A. (2017). A finite area scheme for shallow granular flows such as avalanches. In *OpenFOAM workshop.*

Sovilla, B., McElwaine, J. N., and Köhler, A. (2018). The intermittency region of powder snow avalanches. *J. Geophys. Res.*

Steinkogler, W., Gaume, J., Löwe, H., Sovilla, B., and Lehning, M. (2015). Granulation of snow: From tumbler experiments to discrete element simulations. *J. Geophys. Res.*

Vriend, N. M., McElwaine, J. N., Sovilla, B., Keylock, C. J., Ash, M., and Brennan, P. V. (2013). High-resolution radar measurements of snow avalanches. *Geophys. Res. Lett.*